PCCP

PAPER

View Article Online
View Journal

Cite this: DOI: 10.1039/c8cp00235e

Solvent-dependent dual fluorescence of the push–pull system 2-diethylamino-7-nitrofluorene†

M. A. B. Larsen,[a] A. B. Stephansen,[b] E. Alarousu,[c] M. Pittelkow,[a] O. F. Mohammed*[c] and T. I. Sølling*[a]

The solvent-dependent excited state behavior of the molecular push–pull system 2-diethylamino-7-nitrofluorene has been explored using femtosecond transient absorption spectroscopy in combination with density functional theory calculations. Several excited state minima have been identified computationally, all possessing significant intramolecular charge transfer character. The experimentally observed dual fluorescence is suggested to arise from a planar excited state minimum and another minimum reached by twisting of the aryl–nitrogen bond of the amino group. The majority of the excited state population, however, undergo non-radiative transitions and potential excited state deactivation pathways are assessed in the computational investigation. A third excited state conformer, characterized by twisting around the aryl–nitrogen bond of the nitro group, is reasoned to be responsible for the majority of the non-radiative decays and a crossing between the excited state and ground state is localized. Additionally, ultrafast intersystem crossing is observed in the apolar solvent cyclohexane and rationalized to occur *via* an El-Sayed assisted transition from one of the identified excited state minima. The solvent thus determines more than just the fluorescence lifetime and shapes the potential energy landscape, thereby dictating the available excited state pathways.

Received 11th January 2018,
Accepted 30th January 2018

DOI: 10.1039/c8cp00235e

rsc.li/pccp

Introduction

Dual fluorescence is an intriguing phenomenon exhibited by certain aromatic push–pull chromophores, which seemingly is in violation of Kasha's propensity rule[1] as fluorescence from two excited states are observed. A puzzling aspect is that two fluorescence bands can be observed even when the excitation energy only is sufficient to excite the (vertically) lowest excited state; the situation is thereby different from the one in *e.g.* azulene in which both excitation to and fluorescence from a higher excited state is observed.[2,3] No guidelines exist to design molecules possessing dual fluorescence as the phenomenon can arise from fairly different molecular species. In most cases[4] dual fluorescence is not formally in violation of Kasha's rule as fluorescence does occur from the lowest excited state of a particular conformation; if the fluorophore undergoes a structural rearrangement on the excited state surface this may lead to two excited state minima and two fluorescence bands.

The study of dual fluorescence was originally initiated by a serendipitous discovery in the structurally simple molecule 4-dimethylaminobenzonitrile (4-DMABN),[5,6] and has now been observed in hundreds of systems.[7–10] The insights gained from the many studies has led to a phenomenological understanding of locally excited state and charge transfer (CT) processes which can be applied to *e.g.* retinal, the absorbing moiety of the visual process, and the charge separation occurring in the photosystems of green plants.[8,9,11] Yet, the relative stabilities of the locally excited and CT states depend crucially on interactions with the environment in a complex and sparsely understood manner. The systems studied here have no direct link to biological systems (*i.e.* they are not subunits of known biomolecules) but represent an example in which the solvent-dependent excited state behaviour can be unravelled and rationalized in terms of quantum chemical calculations.

One major recognition is the essential role of twisted intramolecular charge transfer (TICT) processes, which typically are influenced by the molecular environment, *e.g.* pH, temperature, and solvation. TICT processes, however, do not explicitly involve the solvent as part of the excitation but are inherent to the molecule itself, as opposed to *e.g.* solute–solvent exciplexes.[12–14] Solvation may instead influence whether the excited state species becomes more or less stable in a twisted geometry relative to

[a] Department of Chemistry, University of Copenhagen, Universitetsparken 5, DK-2100 Copenhagen Ø, Denmark. E-mail: theis@chem.ku.dk
[b] Department of Molecular Physics, Fritz-Haber Institute of the Max-Planck Society, Faradayweg 4–6, 14195 Berlin, Germany
[c] KAUST Solar Center, Division of Physical Sciences and Engineering, King Abdullah University of Science and Technology (KAUST), Thuwal 23955-6900, Kingdom of Saudi Arabia. E-mail: omar.abdelsaboor@kaust.edu.sa

† Electronic supplementary information (ESI) available: Calculated excited state orbitals, transients, fits, and NMR spectra. See DOI: 10.1039/c8cp00235e

the planar geometry due to a combination of specific, non-specific and possible cooperative solvent effects.[10] One consequence of the solvent dependence is that each molecular system possessing dual fluorescence is unique[4–27] and cannot all be explained solely by a TICT mechanism. Also, numerous systems with structural equivalences do not necessarily exhibit corresponding properties. The lack of a link between structure and dual fluorescence properties is exemplified by 4-DMABN,[5,6] exhibiting dual fluorescence but 4-methylaminobenzonitrile (4-MABN) and 3-dimethylaminobenzonitrile (3-DMABN) only exhibit a single fluorescence band even in polar solvents.[28] 4-MABN and 3-DMABN only differ from 4-DMABN by a single methyl group or the position of the amino group relative to the nitrile group respectively, yet they do not share the dual fluorescence property. The acceptor-π-donor motif shared by the above mentioned systems is present in many other dual fluorescing or non-fluorescing molecules, but it was early on recognized that simply changing the donor or acceptor substituents may also change the ability to exhibit dual fluorescence.[29]

Here, we investigate one of the fundamental aspects of dual fluorescence, namely the impact of the solvent on the potential energy surface (PES), in particular the position of a conical intersection (CI) on the PES as a function of solvent polarity. The primary species under investigation, 2-diethylamino-7-nitrofluorene (de-ANF), displays a single fluorescence band in cyclohexane, but dual fluorescence from two CT type states in polar solvents such as acetonitrile and methanol. The fluorescent state in cyclohexane and the two CT states populated in polar solvents were characterized previously with fluorescence measurements.[30] Here we assess the mechanism for formation of the two CT states by considering the role of twisting either the electron donor (amino) or acceptor (nitro) moiety; both have independently been argued to be responsible for the anomalous fluorescence band emissive state in the analogous 2-dimethylamino-7-nitrofluorene (dm-ANF)[31,32] – see Fig. 1 – other contributions argue that no twisting occurs at all (and that dm-ANF does not display dual fluorescence),[33,34] which seemingly contradicts our previous fluorescence measurements on de-ANF[30] and potentially suggests that the excited state methyl and ethyl conformers are qualitatively different. The main objectives of the present study are thus to identify the role of different excited state minima in de-ANF, establish any qualitative similarities between de-ANF and dm-ANF and in particular assess the "missing" dual fluorescence in the non-polar solvent cyclohexane. The investigation is performed using femtosecond transient absorption (TA) spectroscopy to probe the dynamics and follow interconversion from the initially excited state. This approach gives information about the ground and fluorescent states at the same time. Experiments are performed in three solvents (methanol, acetonitrile and cyclohexane) and the results are supported by time-dependent density functional theory (TD-DFT) calculations to identify the structural changes associated with the dynamics as well as changes in the available relaxation pathways as a function of solvent properties.

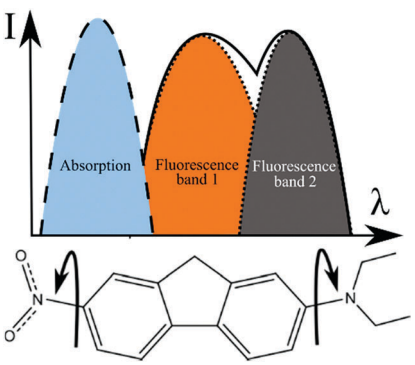

Fig. 1 Schematic representation of dual fluorescence (top): the absorption (blue, broken line) and dual fluorescence (solid line) with the two distinct underlying bands shown (dotted lines). The molecular species (bottom) under investigation, 2-diethylamino-7-nitrofluorene (de-ANF), with the key torsional coordinates illustrated.

Experimental

de-ANF was purchased from Sigma-Aldrich (98%) and purified by chromatography on silica to yield the analytically pure material, and dm-ANF molecules were synthesized as described in literature.[35] Purification of dm-ANF was difficult, but achieved by repeated chromatography on silica, to yield the analytically pure material. NMR spectra of the pure compounds are presented in the ESI† (Fig. S6–S9).

Time-resolved transient absorption (TA)

The setup for femtosecond transient absorption (Helios, Ultrafast Systems, USA) has been described in detail previously[36] and will only be briefly outlined here. 800 nm pulses from an amplified Ti:Sapphire laser system with a 35 fs pulse width at 1 kHz repetition rate were used to generate the white light probe in CaF_2 and sapphire crystals. The white light was then split in two paths; one passing through the cuvette with the sample and one going directly to a reference spectrometer to measure fluctuations in the white light intensity. The pump pulses were generated from an Optical Parametric Amplifier (Topas-C, Light Conversion, Lithuania), chopped to 500 Hz and overlapped with the white light in the cuvette. The sample was kept in a cuvette with a stirring magnet ensuring continuous refreshing of the excited sample, furthermore the datasets have been corrected for the white light spectral chirp from measurements on pure solvent. The nano- and microsecond dynamics were measured using a broad-band pump–probe subnanosecond transient absorption spectrometer with an extended time window (EOS, Ultrafast Systems, USA).

UV/Vis spectroscopy

The steady-state absorption spectra of de-ANF and dm-ANF in methanol were obtained from a diluted sample, down to 10^{-5} M equivalent of an absorption below 0.05. The absorption spectra were recorded on a Cary 50 Spectrometer, the fluorescence and excitation spectra of the same samples were obtained on a Cary Eclipse Fluorescence Spectrophotometer.

Computational

The calculations were performed using Gaussian09,[37] both for the *in vacuo* and polarizable continuum (PCM) solvent calculations as implemented by the PCM keyword using the integral equation formalism model (IEFPCM). We employed PBE0/6-311+G(d,p) for consistency with previous studies, and because this level of theory was found to describe the excited state properties of de-ANF reasonably well.[30] Minimum energy structures (zero imaginary frequencies) were first optimized on the ground state. Excited state minima were then identified by optimization from ground state initial guesses with the planes defined by CNC and ONO being perpendicular to the aromatic skeleton and in same plane, respectively. The potential energy surface was explored with the aim of mapping potential crossing points between the ground and first excited state. We employed a linear interpolation scheme involving extension of the NO bonds, the C–NO_2 bond and the C–NH_2 bond. The linear interpolation was performed by dividing the bond length, bond angle and dihedral angle differences between the start and end geometries by the total number of steps, the increments are added sequentially to generate an array of geometries that are systematically connected.

Results and discussion

The steady-state absorption and fluorescence spectra of de-ANF and dm-ANF in methanol are shown in Fig. 2; the blue lines correspond to measured absorption and the orange lines to fluorescence. The structures of the compounds are given in the upper right corner of the graphs and two Gaussian bands for the two fluorescence bands are given as a guide to the eye. The fluorescence signal in the region from 745–775 nm is removed in both spectra as the second harmonic of the excitation wavelength (380 nm) dominated the signal in this region. The long-wavelength region of the fluorescence resulting from excitation at 450 nm is given in ESI† Fig. S1, exhibiting a band identical to the spectrum given in Fig. 2. It is clear that both compounds show two distinct fluorescence peaks of similar width and intensity. For de-ANF the maxima of the two fluorescence bands are at about 620 nm and 720 nm, while the maxima for dm-ANF are at 610 nm and 720 nm. We note that these values are not from a Gaussian deconvolution but merely represent the maxima values – deconvolution in a series of solvents has been published previously.[30] The spectrum of dm-ANF in methanol has not been reported previously, although a peak absorption wavelength has been reported for this compound at 420 nm[38] and 432 nm.[34] Methanol was chosen as the solvent to illustrate the similarity of the steady-state spectra because the separation of the two fluorescence bands is clearest in this solvent.[30] The fluorescence quantum yields are very low (on the order of 10^{-3}–10^{-4}) and scattering from the solvent is therefore prominent in the obtained spectra. The concentration is kept low to ensure negligible reabsorption effects and excitation spectra for dm-ANF (ESI,† Fig. S2) confirm that the absorbing and emissive species are related. The absorption, fluorescence and excitation spectra of de-ANF in several solvents including acetonitrile, methanol and cyclohexane have been reported previously;[30] notably de-ANF only shows a single fluorescence peak in cyclohexane but dual fluorescence in all other explored solvents. The time-resolved experiments on de-ANF was also performed in acetonitrile solution to substantiate that hydrogen bonding between the solvent and the solute is not a necessity to observe dual emission, although hydrogen bonding may influence the energy of the CT state.

Transient absorption (TA) experiments

Femtosecond transient absorption experiments of de-ANF are performed in three solvents with differing polarity, namely; methanol, acetonitrile and cyclohexane. Measurements are done with two different white light generation crystals, resulting in two different but overlapping spectra. The resulting transient spectra (Fig. 3) represent difficult datasets to analyze due to spectral shifts and overlapping features of different species, and we therefore limit ourselves to a semi-quantitative analysis with the primary timescales obtained from bands with no (or minimal)

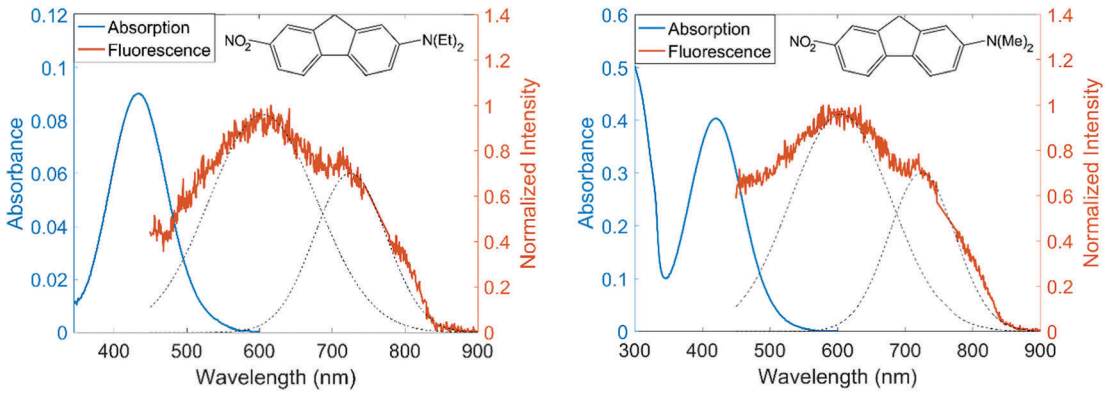

Fig. 2 Steady-state absorption and fluorescence spectra of de-ANF in methanol (left) and dm-ANF in methanol (right) at room temperature, excited at 380 nm. The concentrations are on the order of 10^{-5} M for both molecules. Only a few counts were observed at each data point as the fluorescence intensity is very weak. Note that the region from 745–775 nm is removed as the second order signal from the excitation wavelength (380 nm) dominates the signal in this spectral region. Gaussians are only given as a guide to the eye to distinguish the two fluorescence peaks (broken line).

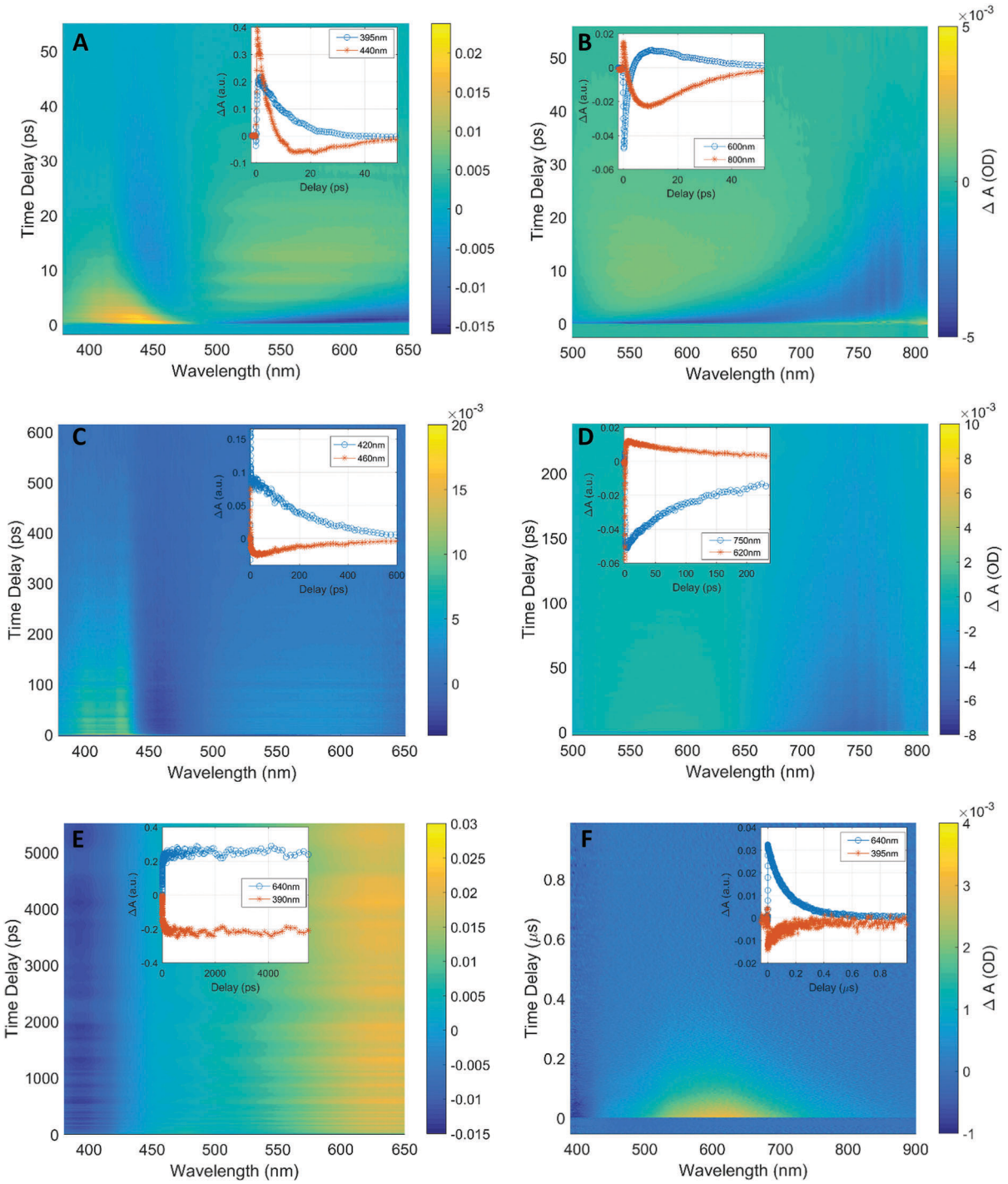

Fig. 3 Transient absorption measurements in methanol (A and B), in acetonitrile (C and D) and in cyclohexane (E and F) showing the ground state bleach (in the blue region), excited state absorption in yellow color and stimulated emission in the 700–800 nm region. Insets show transients at specific wavelengths relating to ground state bleaches, ESA and SE bands.

overlapping features. There is no exclusive way to globally fit the data, which was also noted previously in the analysis of TA spectra of dm-ANF,[34] and the assignments are therefore closely linked with the steady-state absorption spectra and guided qualitatively by the theoretically identified excited state minima. The fits of the transients are given in ESI† Fig. S3 and although the exact timescales cannot be trusted (*i.e.* quantitative information), the dynamics in the different solvents are sufficiently different (tens of ps, hundreds of ps and hundreds of ns), that information about the order of magnitude (*i.e.* semi-quantitative information) is clear. Additionally, the qualitative behaviour is sufficiently different that considerable information can be gathered from the experimental spectra. In the short wavelength region of the TA spectra of de-ANF in methanol (Fig. 3A), a positive signal

(*i.e.* excited state absorption (ESA) (yellow in the spectrum)) in the spectral range from 390 nm to 475 nm overlaps with a negative signal (*i.e.* ground state bleach or stimulated emission (SE) (blue in the spectrum)). The inset shows a representative kinetic trace for the positive signal at 395 nm (blue line with circles) and a trace at 440 nm (orange line with stars), which shows the recovery of the negative signal. Both the positive and the negative signal have returned to zero after 50 ps. In the long wavelength region (Fig. 3B) a positive signal is present from 500 nm to 700 nm with an initial negative signal preceding the positive signal. Beyond 750 nm, the signal remains negative and a trace at 800 nm is shown in the inset, along with a trace at 600 nm. Similar to the short wavelength measurements, the negative and positive signal return to zero after 50 ps.

The short wavelength region of the TA spectra of de-ANF in acetonitrile (Fig. 3C) is qualitatively similar to the data observed for de-ANF in methanol: a positive signal is observed from 390 nm to 440 nm, a negative signal is present from 445 nm to 480 nm and another positive signal is observed from 500 nm to 650 nm. The inset shows traces at 420 nm (the short wavelength positive band) and at 460 nm (the negative band). Both features have returned to zero after 600 ps. In the long wavelength region for acetonitrile (Fig. 3D), the similarity to methanol is again striking: a positive band preceded by a very short lived negative signal is present from 500 nm to 700 nm and a simple negative signal is observed beyond 700 nm – the negative signal preceding the ESA and the similarity to the behaviour in methanol can be clearly seen at short time delays (ESI,† Fig. S4).

In Fig. 3E and F, the TA spectra of de-ANF in cyclohexane are shown and now a very different behaviour is observed: only two bands are present, a negative band and a very broad positive band. It should be noted that the timescales are different in Fig. 3E and F; the 5 ns traces in Fig. 3E of the negative and positive signals show no decay, but the μs traces in Fig. 3F show return of both traces to zero. Fitting an exponential decay to the microsecond experiment reveals a 140 ns lifetime of the two bands, many orders of magnitude longer than any timescale previously observed for dm-ANF or de-ANF in any solvent. Based on the steady-state absorption spectrum, the negative signal in the TA spectrum is assigned to a ground state bleach and the positive band to absorption by a long-lived excited state of de-ANF. The most likely candidate for this long-lived excited state species is a triplet state,[39] similar to what has been observed in nitro-aromatic compounds.[40–45] An alternative scenario would be the formation of a photoproduct;[46–48] however this would not result in a concomitant rise on the μs timescale of the ground state bleach, as is observed in the current data. The formation of a triplet state provides a non-radiative excited state deactivation mechanism for the initially excited singlet state and more importantly, illustrates how the solvent impacts the PES and completely changes the photophysics in cyclohexane compared to the polar solvents. Partial recovery of the ground bleach of de-ANF in cyclohexane is also seen on a much shorter timescale of about 8 ps and 100 ps, the latter of which is in agreement with the fluorescence lifetime of the compound measured previously[30] while the former has not been reported before and will be discussed later on.

In the polar solvents, methanol and acetonitrile, the observed features are qualitatively similar and assignments of the observed bands in both solvents are likely to be the same. They will therefore be discussed together in the following. The similarity is not expected *a priori* as the different dielectric constants and the introduction of hydrogen bonding effects could induce large changes to the excited state PES. Also, some difference is clear from the lifetimes that differ by an order of magnitude in methanol compared to acetonitrile.

The short wavelength bleaches are assigned to the ground state bleaches based on the steady-state absorption spectra. The long-wavelength bleaches are assigned to the second fluorescence bands, again due to spectral match with the steady-state spectra and the bleaches beyond 750 nm are thus assigned to be SE bands. The short wavelength ESA bands appear within the cross-correlation of our setup and are assigned to an excited state minimum and tentatively ascribed the state associated with the short wavelength fluorescence peak. The short wavelength fluorescence from the steady-state spectra is only observed briefly as an SE band, before the long wavelength ESA band rises. These second ESA bands, with distinct rising times, are tentatively assigned to the excited state minimum associated with the long wavelength fluorescence band, *i.e.* likely a singlet excited state as elaborated later on.

The timescales of the dynamics in methanol are obtained from fits to the experimental data (ESI,† Fig. S3) and indicate that all four observed bands have a similar overall lifetime of $\sim$20 ps. The long wavelength ESA band and SE band both have a 3–4 ps rise time and the short wavelength ESA band has a corresponding 3–4 ps decay component. These observations indicate an equilibration between the two excited state minima and parallel deactivation of the excited states.

The short wavelength ESA band in acetonitrile is tentatively attributed to the excited state responsible for the short wavelength fluorescence band as the band appears within the cross-correlation. A short-lived SE band matching the short wavelength fluorescence is also observed (ESI,† Fig. S4) before the long wavelength ESA rises – similar to the bands in methanol. The band at 445–480 nm is assigned as ground state bleach, matching the absorption spectrum and the long wavelength SE band is assigned to second emissive state with an ESA from 500–650 nm. The qualitative features of de-ANF in acetonitrile are thus identical to the ones in methanol but the decays are much slower compared to the dynamics in methanol. The decay of the excited states is described by two timescales; a 30–50 ps component and a slower 180 ps decay. The latter of which is observed in all 4 observed bands and matches the previously obtained time constants from fluorescence up-conversion measurements in acetonitrile.[30] The interconversion timescale between the emissive states, however, is much faster than the 3–4 ps in methanol: the long wavelength SE band shows a rise time of 0.5–0.8 ps, which is matched by a 0.5–0.8 ps decay component in the short wavelength bands. The 30–50 ps timescale may be related to slower solvation effects or more likely a sub-population of vibrationally excited, potentially ethyl-chain conformers of de-ANF undergoing deactivation parallel to the

majority of the population. However, the exact mechanism behind this remains speculative and is not discussed further.

Summing up, the interconversion timescale and lifetime from the fluorescence up-conversion measurements (for de-ANF in acetonitrile and cyclohexane) agree well with lifetimes of the singlet excited states obtained here, affirming the quality of the fits. The matching dynamics of the assigned ESA bands corroborate that the observed bands in fact corresponds to the emissive states and the notion of interconversion between the emissive states suggested from the fluorescence up-conversion experiments. The TA measurements also adds several new pieces of information to the investigation into the dynamics of de-ANF, most prominently the very long-lived excited state observed in cyclohexane.

Briefly considering dm-ANF, the position and timescales of the bands from de-ANF in methanol match the previously published results for dm-ANF in methanol well, both the short wavelengths bands[33,34] and the long wavelength bands.[31] The TA measurements thus substantiate a close similarity between de- and dm-ANF, as established in the steady-state fluorescence measurements. The quantum chemical investigation in the following sections further corroborate this close similarity between de- and dm-ANF.

Excited state minima

An initial analysis of the ground state conformations of de-ANF resulted in 7 minima with different orientations of the ethyl moieties linked to the amino group (ESI,† Fig. S2). The excitation energies varied only slightly (within 0.04 eV) and the relative energies indicate that a single conformer constitutes 71% of the ground state population at room temperature, all further calculations on de-ANF will therefore be restricted to this single conformer (ESI,† Table S1).

Three different excited state minima are identified *in vacuo* for both dm-ANF and de-ANF with the de-ANF structures shown in Fig. 4; a planar minimum (S_{1P}), a minimum with a rotated amino group (S_{1A}), and a minimum with a rotated and pyramidalized nitro group (S_{1N}). The relative energies of the minima are given in Table 1. The structures of the minima are qualitatively similar to previously suggested excited state minima for dm-ANF[32] but are the first excited state minimum energy structures reported for de-ANF. The minima are close in energy and will therefore all be considered when analysing the excited state dynamics. For de-ANF the small energy differences between the excited state minima represent a particular challenge as the ethyl conformers identified in the ground state adds several shallow minima separated by small (rotational) barriers. The 3 de-ANF excited state minima all correspond to the minimum energy ground state ethyl conformer.

The S_{1P} and S_{1A} minima are almost equivalent in energy, differing only by 0.02 eV in the case of dm-ANF and by 0.07 eV in the case of de-ANF. Their role in the dual fluoresence will be discussed shortly but first the S_{1N} minimum is considered: the energy of the S_{1N} minimum is actually considerably lower in energy (0.17–0.22 eV) than the S_{1P} and S_{1N} minima and one therefore might expect relaxation towards this minimum. Despite this, S_{1N} is excluded as a potential source of fluorescence and the role of relaxation to the S_{1N} is discussed in detail in Section 2.3. The exclusion of S_{1N} as a fluorescent minimum can be understood by comparing experimental and calculated Stokes shifts.

The calculated Stokes shift associated with the S_{1N} conformer of dm-ANF is 1.78 eV, whereas the largest experimental Stokes shift is 1.22 eV (taken as the difference between the maxima of the absorption peak and longest wavelength fluorescence peak). For de-ANF the largest experimental shift is 1.15 eV and the S_{1N} calculation predicts a shift of 2.14 eV. An overestimation of the Stokes shift by almost 1 eV from an *in vacuo* calculation that otherwise reproduces the excited state energies reasonably well – see Table 2 – indicates that it is unlikely that the S_{1N} conformer is responsible for any of the fluorescence peaks observed in polar solvents. Additionally, twisting of the nitro-group may lead to efficient relaxation to the ground state (*vide infra*) or NO• release,[44,45] which is not observed in the current experiment. By comparison both the S_{1P} and S_{1A} conformers of dm-ANF underestimate the Stokes shift by 0.3–0.7 eV.

Clearly, solvation of the molecular species plays a role as witnessed by the lack of a second fluorescence band of de-ANF in cyclohexane. Optimization of excited state minima using a polarizable continuum model (PCM) has also been attempted based on the *in vacuo* structures but it was only possible to converge the S_{1P} and S_{1N} minima for both dm-ANF and de-ANF. The calculated fluorescence energies for the S_{1P} and S_{1A} dm-ANF minima are given in Table 2 and match the experimental fluorescence energies quite well. Since optimization of the S_{1A} minimum for de-ANF was not successful (potentially related to the existence of many ethyl conformers), the assignment of the S_{1A} minimum in de-ANF as an emissive species relies on the close correspondence between the excited states of dm-ANF

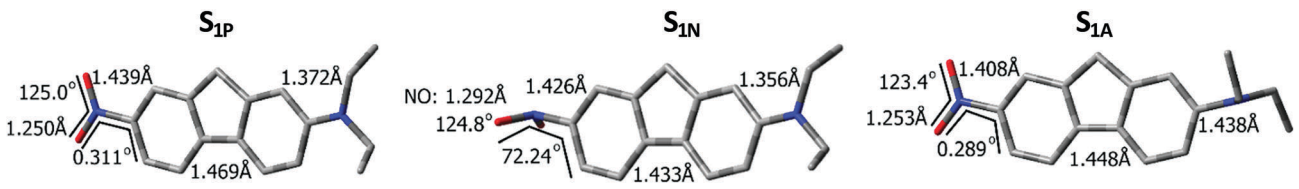

Fig. 4 Calculated structures (PBE0/6-311+G(d,p)) of the three different minima located on the excited state (hydrogens not shown) with selected geometrical parameters given for the planar S_{1P} local minimum (left), the S_{1N} minimum with the rotated and pyramidalized nitro group (middle) and the S_{1A} minimum with a rotated amino group (right).

Table 1 Gas phase excited state energies (in eV) of dm-ANF and de-ANF ((TD)-PBE0/6-311+G(d,p))

	dm-ANF	de-ANF
S_0	0	0
FC S_1	3.08	3.04
S_{1P}	2.89	2.93
S_{1N}	2.72	2.71
S_{1A}	2.91	3.00
S_0–S_1 crossing	—	3.07

Table 2 Calculated and experimental fluorescence energies in eV. The relative energy to the S_{1P} state is given in the parentheses (TD-PBE0/6-311+G(d,p)/PCM)

	dm-ANF exp	dm-ANF calc, MeOH	de-ANF exp	de-ANF calc, MeOH
S_{1P}	2.03	2.20 (0)	2.00	2.17 (0)
S_{1N}	—	0.94 (−0.047)	—	0.89 (−0.096)
S_{1A}	1.72	1.70 (+0.303)	1.72	—

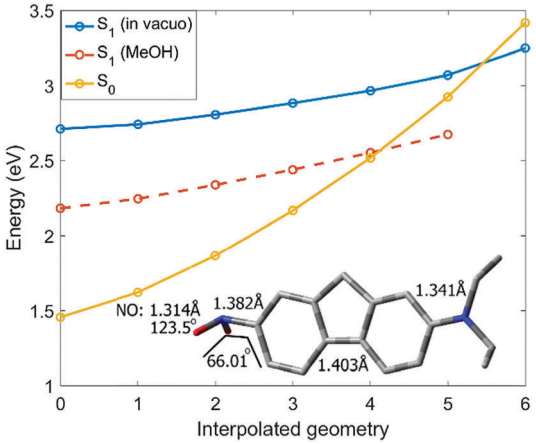

Fig. 5 Geometries linearly interpolated from the de-ANF S_{1N} minimum across the S_0/S_1 crossing point (structure given in inset). The S_0 curve for the PCM calculation is not reproduced as is within 0.05 eV of the *in vacuo* calculation (TD-PBE0/6-311+G(d,p) *in vacuo*/PCM(methanol)).

and de-ANF: the steady-state fluorescence spectra are very similar, only the positions of the peaks shift slightly. The calculated relative energies are also very comparable for both *in vacuo* and PCM calculations, yielding similar values for the S_{1P} and S_{1N} fluorescence energies in dm-ANF and de-ANF. Given these correlations, extending the similarity from the *in vacuo* S_{1A} minima to the PCM calculations seems plausible.

The energies of S_{1A} and S_{1N} conformers relative to the planar S_{1P} conformer are given in parentheses in Table 2 and show that the effect of the polar solvent model mainly is to reduce the energy difference between the excited state minima; the energy difference between the S_{1P} and S_{1N} conformers is reduced to half of the gasphase values. In general, the S_{1A} conformer proved more difficult to optimize with the PCM and in most attempts resulted in optimization of a transition state (even for dm-ANF). This could indicate a contourless PES with a very small or no barrier for interconversion between the two excited state minima.

Excited state deactivation

The previous work on dm-ANF[31–34]/de-ANF[30] and discussion so far have been focused on the fluorescent states as they are immediately observable in the steady-state spectra. However, as already noted the fluorescence quantum yields in methanol and acetonitrile are only on the order of 10^{-3}–10^{-4} and more than 99% of the excited molecules must undergo some non-radiative process. In cyclohexane the fluorescence quantum yield is larger (2.5×10^{-2}) but 97.5% of the molecules still do not fluoresce.[30] Internal conversion (IC) mediated by a conical intersection between the excited state and the ground state could explain the efficient deactivation of the excited state. The small energy gap between the S_{1N} conformer and the ground state makes the S_{1N} conformer an obvious starting point for a search of a conical intersection. The calculated PES shown in Fig. 5 (TD-PBE0/6-311+G(d,p)/PCM, ground state energies taken as zero-point) reveals a crossing point between the ground and excited states for de-ANF along a linear interpolation coordinate between the already rotated and pyramidalized S_{1N} minimum and a perturbed structure (given in Fig. 5). The end-point is closely related to the S_{1N} conformer, but has slightly longer NO bonds, a slightly shorter C–NO_2 bond and a slightly longer C–NH_2 bond. The calculations summarized in Fig. 5 show a minor increase in the excited state energy but a large increase in ground state energy associated with the structural changes.

Note that only a single ground state (S_0) line is drawn in Fig. 5; this is because the *in vacuo* and PCM (MeOH) ground state calculations differ by less than 0.05 eV and only the *in vacuo* ground state PES is therefore shown in the figure. The primary effect of the solvent is thus to stabilize the excited states and this effect can be expected to be just as relevant in acetonitrile. The methanol PCM calculation in Fig. 5 exemplifies the stabilization of the excited state. Additionally, it reveals that the S_1–S_0 crossing is associated with a smaller structural change in the polar solvent compared to the *in vacuo* calculation. This is consistent with an even more efficient IC to the ground state in the polar solvents compared to cyclohexane. Even in the *in vacuo* calculations the S_1–S_0 CI can be reached solely from the FC excitation energy without any additional vibrational excitation – see Table 1. The crossing can thus be expected to be active in all three solvents, mediating an efficient non-radiative deactivation pathway for the excited state.

Intersystem crossing (ISC)

The experimental ESA for de-ANF in cyclohexane shows that three different timescales are involved; an 8 ps, a 100 ps and a 140 ns component. The 100 ps component matches the fluorescence lifetime[30] and the slow component of the ESA matches a concomitant rise of the ground state bleach, thereby indicating involvement of a triplet state which eventually returns to the ground state. The 8 ps component is likely related to the triplet state as it wasn't observed in previous fluorescence experiments and would be explained by IC within the triplet manifold. A similar timescale for IC within the triplet manifold has been reported for the analogous nitro-compound without an amino-group.[40]

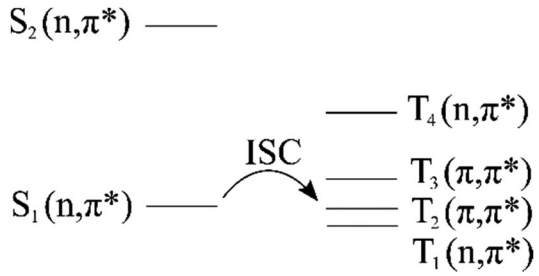

Fig. 6 Energetics and principal character of the excitations of de-ANF in the S_{1A} minimum structure (TD-PBE0/6-311+G(d,p)/*in vacuo*).

The ESA band appears within the cross-correlation and hints that the fluorescent state as well as the initial triplet state is populated ultrafast. The previous fluorescence study of de-ANF could not observe triplet states and calculations at the FC structure indicated that ISC did not take place.

In addition to the proposed triplet state, de-ANF in cyclohexane lacks the long wavelength fluorescence band exhibited in polar solvents. However, the *in vacuo* calculations indicate that all three excited state minima are close in energy and the role of the excited state minimum assigned as the long wavelength fluorescence emissive state in the polar solvents (S_{1A}), must be reconsidered.

The first few singlet and triplet states, along with their characters are summarized in Fig. 6 for the S_{1A} minimum structure. As indicated in the figure, the S_{1A} minimum in fact appears to be a prominent candidate for an efficient ISC pathway in cyclohexane: an El-Sayed type assisted ISC from S_1 to T_2 is not available at the FC structure but opens up in the S_{1A} minimum. Furthermore, the energy gap between the interacting singlet and triplet states is essentially zero (ΔE = 0.001 eV). An ultrafast ISC process, happening on a sub 100 fs timescale, has been shown to occur in other nitro containing aromatic compounds[40–45,49–56] and could explain the appearance of the ESA band for de-ANF in cyclohexane, despite our previous assumption that the ISC channel was closed for de-ANF.[30] However, no ISC is apparent in the dynamics observed in the polar solvents. Indeed, our calculations indicate that the T_2 state is no longer accessible in methanol (PCM); adding the methanol solvent results in a significant stabilization of the S_{1A} conformer relative to the T_2 state and the T_2 is thus significantly higher in energy in the polar solvent. Since no S_{1A} minimum could be found for de-ANF with PCM, these observations are based on calculations on dm-ANF. These show that the S_{1A} conformer is stabilized 0.3 eV more than the T_2 state when a methanol PCM is added, indicating that the ISC pathway simply is inaccessible in the polar solvents.

The TA spectra thus not only corroborates the fluorescence lifetime from previous measurements, but reveals dynamics several orders of magnitudes slower than has previously been reported for either dm-ANF or de-ANF.

Fig. 7 shows a summarizing overview of the suggested structural changes and processes associated with the different excited state minima. The dynamics following excitation to the Franck–Condon (FC) geometry is dominated by IC to the ground state *via* the S_{1N} minimum and a crossing point with the ground state has been located. In polar solvents this crossing point with the ground state requires less structural rearrangement, which supports the experimental finding of a lower fluorescence quantum yield in the polar solvents. The dual fluorescence bands are explained in terms of a planar S_{1P} minimum and a S_{1A} minimum with a rotated amino group. The experiments indicate equilibration between the two states and parallel deactivation, which is supported by calculations showing the two states to be essentially isoenergetic. The fluorescence energies calculated with PCM are in good agreement with the experimentally observed bands (Table 2). In apolar cyclohexane, the dynamics are vastly different; while the planar S_{1P} is still responsible for the fluorescence band, the S_{1A} minimum now leads to ultrafast ISC. Still, the majority of the population is efficiently deactivated through the located S_1–S_0 CI.

Conclusions

The strongly solvent-dependent excited state dynamics of the push–pull molecule de-ANF has been investigated by femtosecond transient absorption spectroscopy and supported by DFT calculations. The polarity of the solvent is shown to change the state ordering and thereby heavily influence the nature of the resulting dynamics. Interestingly, ISC is observed in nonpolar cyclohexane along with a single emissive state, whereas two fluorescent states and no ISC is observed in the polar solvents methanol and acetonitrile.

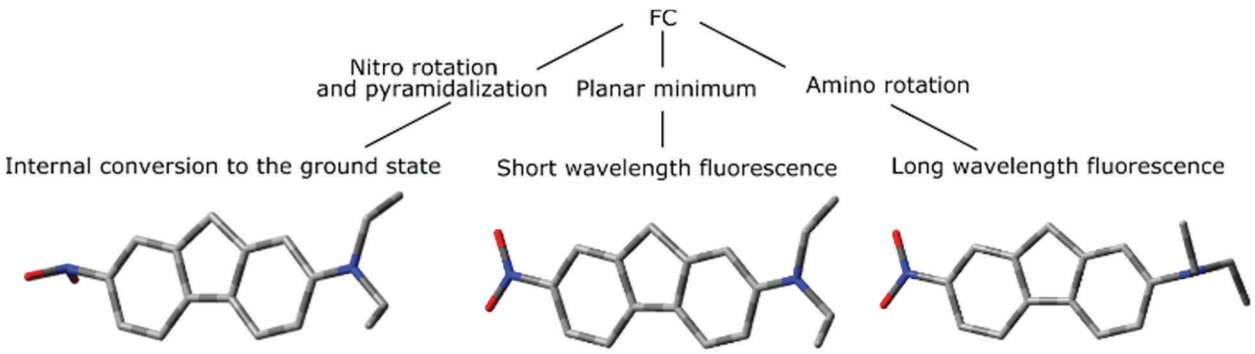

Fig. 7 An overview of the proposed deactivation mechanisms and the relevant optimized structures of de-ANF.

The S_{1P} planar minimum and the S_{1A} twisted amino minimum are the emissive states in polar solvents. In cyclohexane, no dual fluorescence is observed as the solvent modifies the PES and state-ordering, so that the S_{1A} minimum leads to efficient ISC and the formation of the triplet state that eventually returns to the ground state on a hundreds of ns timescale.

The low fluorescence quantum yield in all three solvents is explained by a S_1–S_0 crossing nearby the lowest energy excited state structure, S_{1N}. The position of this crossing is also influenced by the solvent polarity and calculations indicate that a smaller structural change is required in the polar solvents to the reach the crossing, potentially explaining why a lower quantum yield was observed in the polar solvents compared to the non-polar solvent. Still, the interconversion between the excited states responsible for the two emissive states can be followed by the transient absorption experiments and an equilibration between the emissive states followed by parallel deactivation is observed. Collectively this gives a broad overview of the excited state dynamics in dm-ANF and de-ANF.

Conflicts of interest

There are no conflicts to declare.

Acknowledgements

E. A. and O. F. M. gratefully acknowledge funding support from KAUST. Miss Sidsel A. Bogh and Dr Martin Rosenberg are both thanked for their advice and suggestions in obtaining fluorescence spectra of the weakly fluorescent compounds.

Notes and references

1 M. Kasha, *Discuss. Faraday Soc.*, 1950, **9**, 14–19.
2 M. Beer and H. C. Longuet-Higgins, *J. Chem. Phys.*, 1955, **23**, 1390–1391.
3 G. Viswanath and M. Kasha, *J. Chem. Phys.*, 1956, **24**, 574–577.
4 G. Brancato, G. Signore, P. Neyroz, D. Polli, G. Cerullo, G. Abbandonato, L. Nucara, V. Barone, F. Beltram and R. Bizzarri, *J. Phys. Chem. B*, 2015, **119**, 6144–6154.
5 E. Lippert, *Z. Elektrochem.*, 1957, **61**, 962–975.
6 E. Lippert, W. Lüder, F. Moll, W. Nägele, H. Prigge and I. Seibold-Blankenstein, *Angew. Chem.*, 1961, **73**, 695–706.
7 E. Lippert, W. Rettig, V. Bonacickoutecky, F. Heisel and J. A. Miehe, *Adv. Chem. Phys.*, 1987, **68**, 1–173.
8 W. Rettig, *Angew. Chem., Int. Ed. Engl.*, 1986, **25**, 971–988.
9 W. Rettig, *Angew. Chem.*, 1986, **98**, 969–986.
10 Z. R. Grabowski, K. Rotkiewicz and W. Rettig, *Chem. Rev.*, 2003, **103**, 3899–4031.
11 W. Rettig, *Proc. – Indian Acad. Sci., Chem. Sci.*, 1992, **104**, 89–104.
12 E. A. Chandross and H. T. Thomas, *Chem. Phys. Lett.*, 1971, **9**, 397–400.
13 M. C. C. de Lange, D. T. Leeson, K. A. B. van Kuijk, A. H. Huizer and C. A. G. O. Varma, *Chem. Phys.*, 1993, **174**, 425–440.
14 M. C. C. de Lange, D. Thorn Leeson, K. A. B. van Kuijk, A. H. Huizer and C. A. G. O. Varma, *Chem. Phys.*, 1993, **177**, 243–256.
15 Z. R. Grabowski, K. Rotkiewicz and A. Siemiarczuk, *J. Lumin.*, 1979, **18–19**, 420–424.
16 S. Sasaki, G. P. C. Drummen and G.-I. Konishi, *J. Mater. Chem. C*, 2016, **4**, 2731–2743.
17 K. A. Zachariasse, M. Grobys, T. von der Haar, A. Hebecker, Y. V. Ilichev, Y. B. Jiang, O. Morawski and W. Kuhnle, *J. Photochem. Photobiol., A*, 1996, **102**, 59–70.
18 J. Dobkowski, J. Wójcik, W. Koźmiński, R. Kołos, J. Waluk and J. Michl, *J. Am. Chem. Soc.*, 2002, **124**, 2406–2407.
19 R. Hu, E. Lager, A. Aguilar-Aguilar, J. Liu, J. W. Y. Lam, H. H. Y. Sung, I. D. Williams, Y. Zhong, K. S. Wong, E. Peña-Cabrera and B. Z. Tang, *J. Phys. Chem. C*, 2009, **113**, 15845–15853.
20 S. Wiedbrauk, B. Maerz, E. Samoylova, P. Mayer, W. Zinth and H. Dube, *J. Phys. Lett.*, 2017, **8**, 1585–1592.
21 S. Aoki, D. Kagata, M. Shiro, K. Takeda and E. Kimura, *J. Am. Chem. Soc.*, 2004, **126**, 13377–13390.
22 J. L. Zafra, A. Molina Ontoria, P. Mayorga Burrezo, M. Peña-Alvarez, M. Samoc, J. Szeremeta, F. J. Ramírez, M. D. Lovander, C. J. Droske, T. M. Pappenfus, L. Echegoyen, J. T. López Navarrete, N. Martín and J. Casado, *J. Am. Chem. Soc.*, 2017, **139**, 3095–3105.
23 C. Singh, B. Modak, J. A. Mondal and D. K. Palit, *J. Phys. Chem. A*, 2011, **115**, 8183–8196.
24 C. Singh, R. Ghosh, J. A. Mondal and D. K. Palit, *J. Photochem. Photobiol., A*, 2013, **263**, 50–60.
25 M. C. C. de Lange, D. T. Leeson, K. A. B. van Kuijk, A. H. Huizer and C. A. G. O. Varma, *Chem. Phys.*, 1993, **177**, 243–256.
26 E. J. A. de Bekker, A. Pugzlys and C. A. G. O. Varma, *J. Phys. Chem. A*, 2002, **106**, 5974–5988.
27 G. Eber, F. Grüneis, S. Schneider and F. Dörr, *Chem. Phys. Lett.*, 1974, **29**, 397–404.
28 K. A. Zachariasse, *Chem. Phys. Lett.*, 2000, **320**, 8–13.
29 D. J. Cowley and A. H. Peoples, *J. Chem. Soc., Chem. Commun.*, 1977, 352–353, DOI: 10.1039/C3977000352B.
30 R. Lopez-Arteaga, A. B. Stephansen, C. A. Guarin, T. I. Solling and J. Peon, *J. Phys. Chem. B*, 2013, **117**, 9947–9955.
31 J. A. Mondal, M. Sarkar, A. Samanta, H. N. Ghosh and D. K. Palit, *J. Phys. Chem. A*, 2007, **111**, 6122–6126.
32 J. Xia, M. Zhou, S. Sun, G. Wang, P. Song and M. Ge, *Dyes Pigm.*, 2014, **103**, 71–75.
33 V. Karunakaran, T. Senyushkina, G. Saroja, J. Liebscher and N. P. Ernsting, *J. Phys. Chem. A*, 2007, **111**, 10944–10952.
34 V. Karunakaran, M. Pfaffe, I. Ioffe, T. Senyushkina, S. A. Kovalenko, R. Mahrwald, V. Fartzdinov, H. Sklenar and N. P. Ernsting, *J. Phys. Chem. A*, 2008, **112**, 4294–4307.
35 G. Saroja, Z. Pingzhu, N. P. Ernsting and J. Liebscher, *J. Org. Chem.*, 2004, **69**, 987–990.
36 S. M. Aly, G. H. Ahmed, B. S. Shaheen, J. Sun and O. F. Mohammed, *J. Phys. Lett.*, 2015, **6**, 791–795.
37 M. J. Frisch, G. W. Trucks, H. B. Schlegel, G. E. Scuseria, M. A. Robb, J. R. Cheeseman, G. Scalmani, V. Barone, B. Mennucci, G. A. Petersson, H. Nakatsuji, M. Caricato,

X. Li, H. P. Hratchian, A. F. Izmaylov, J. Bloino, G. Zheng, J. L. Sonnenberg, M. Hada, M. Ehara, K. Toyota, R. Fukuda, J. Hasegawa, M. Ishida, T. Nakajima, Y. Honda, O. Kitao, H. Nakai, T. Vreven, J. J. A. Montgomery, J. E. Peralta, F. Ogliaro, M. Bearpark, J. J. Heyd, E. Brothers, K. N. Kudin, V. N. Staroverov, R. Kobayashi, J. Normand, K. Raghavachari, A. Rendell, J. C. Burant, S. S. Iyengar, J. Tomasi, M. Cossi, N. Rega, J. M. Millam, M. Klene, J. E. Knox, J. B. Cross, V. Bakken, C. Adamo, J. Jaramillo, R. Gomperts, R. E. Stratmann, O. Yazyev, A. J. Austin, R. Cammi, C. Pomelli, J. W. Ochterski, R. L. Martin, K. Morokuma, V. G. Zakrzewski, G. A. Voth, P. Salvador, J. J. Dannenberg, S. Dapprich, A. D. Daniels, Ö. Farkas, J. B. Foresman, J. V. Ortiz, J. Cioslowski and D. J. Fox, *Gaussian 09, Revision B.01*, Gaussian Inc., Wallingford CT, 2009.

38 J. Catalan, V. Lopez, P. Perez, R. Martinvillamil and J. G. Rodriguez, *Liebigs Ann.*, 1995, 241–252.

39 O. F. Mohammed and E. Vauthey, *J. Phys. Chem. A*, 2008, **112**, 3823–3830.

40 M. A. B. Larsen, J. Thøgersen, A. B. Stephansen, J. Peon, T. I. Sølling and S. R. Keiding, *J. Phys. Chem. A*, 2016, **120**, 28–35.

41 C. E. Crespo-Hernandez, G. Burdzinski and R. Arce, *J. Phys. Chem. A*, 2008, **112**, 6313–6319.

42 C. E. Crespo-Hernandez, R. A. Vogt and B. Sealey, *Mod. Chem. Appl.*, 2013, **1**, 1000106.

43 C. Reichardt, R. A. Vogt and E. Crespo-Hernandez, *J. Chem. Phys.*, 2009, **131**, 224518.

44 R. A. Vogt and C. E. Crespo-Hernandez, *J. Phys. Chem. A*, 2013, **117**, 14100–14108.

45 R. A. Vogt, C. Reichardt and C. E. Crespo-Hernandez, *J. Phys. Chem. A*, 2013, **117**, 6580–6588.

46 R. Arce, E. F. Pino, C. Valle and J. Agreda, *J. Phys. Chem. A*, 2008, **112**, 10294–10304.

47 O. Cvrckova and M. Ciganek, *Polycyclic Aromat. Compd.*, 2005, **25**, 141–156.

48 Z. I. Garcia-Berrios and R. Arce, *J. Phys. Chem. A*, 2012, **116**, 3652–3664.

49 C. L. Thomsen, J. Thøgersen and S. R. Keiding, *J. Phys. Chem. A*, 1998, **102**, 1062–1067.

50 H. Ohtani, T. Kobayashi, K. Suzuki and S. Nagakura, *Bull. Chem. Soc. Jpn.*, 1980, **53**, 43–47.

51 R. Morales-Cueto, M. Esquivelzeta-Rabell, J. Saucedo-Zugazagoitia and J. Peon, *J. Phys. Chem. A*, 2007, **111**, 552–557.

52 J. S. Zugazagoitia, C. X. Almora-Diaz and J. Peon, *J. Phys. Chem. A*, 2008, **112**, 358–365.

53 J. S. Zugazagoitia, E. Collado-Fregoso, E. F. Plaza-Medina and J. Peon, *J. Phys. Chem. A*, 2009, **113**, 805–810.

54 E. Collado-Fregoso, J. S. Zugazagoitia, E. F. Plaza-Medina and J. Peon, *J. Phys. Chem. A*, 2009, **113**, 13498–13508.

55 E. F. Plaza-Medina, W. Rodriguez-Cordoba, R. Morales-Cueto and J. Peon, *J. Phys. Chem. A*, 2011, **115**, 577–585.

56 E. F. Plaza-Medina, W. Rodriguez-Cordoba and J. Peon, *J. Phys. Chem. A*, 2011, **115**, 9782–9789.

